Supporting Information

Water Confined in Mesoporous TiO_2 Aerosols: Insights from NMR Experiments and Molecular Dynamics Simulations

Manuel I. Velasco,[1] M. Belén Franzoni,[1] Esteban A. Franceschini,[2] Estefanía Gonzalez Solveyra,[3,4] Damián Scherlis,[3,5] Rodolfo H. Acosta*,[1] Galo J. A. A. Soler-Illia*[3,6]

1 FAMAF, Universidad Nacional de Córdoba and IFEG-CONICET, 5016 Córdoba, Argentina

2 INFIQC-CONICET, Dto. de Fisicoquímica – Facultad de Ciencias Químicas, Universidad Nacional de Córdoba, Ciudad Universitaria, 5000, Córdoba, Argentina

3 DQIAQF, Facultad de Ciencias Exactas y Naturales, Universidad de Buenos Aires, Ciudad Universitaria, Pab. II, C1428EHA, Ciudad Autónoma de Buenos Aires, Argentina

4 Department of Biomedical Engineering, Department of Chemistry and Chemistry of Life Processes Institute, Northwestern University, Evanston, IL, United States

5 INQUIMAE, Facultad de Ciencias Exactas y Naturales, Universidad de Buenos Aires, Ciudad Universitaria, Pab. II, C1428EHA, Ciudad Autónoma de Buenos Aires, Argentina

6 Instituto de Nanosistemas, Universidad Nacional de General San Martín, Av. 25 de Mayo y Francia, 1650, San Martín, Argentina

*corresponding authors: racosta@famaf.unc.edu.ar; gsoler-illia@unsam.edu.ar

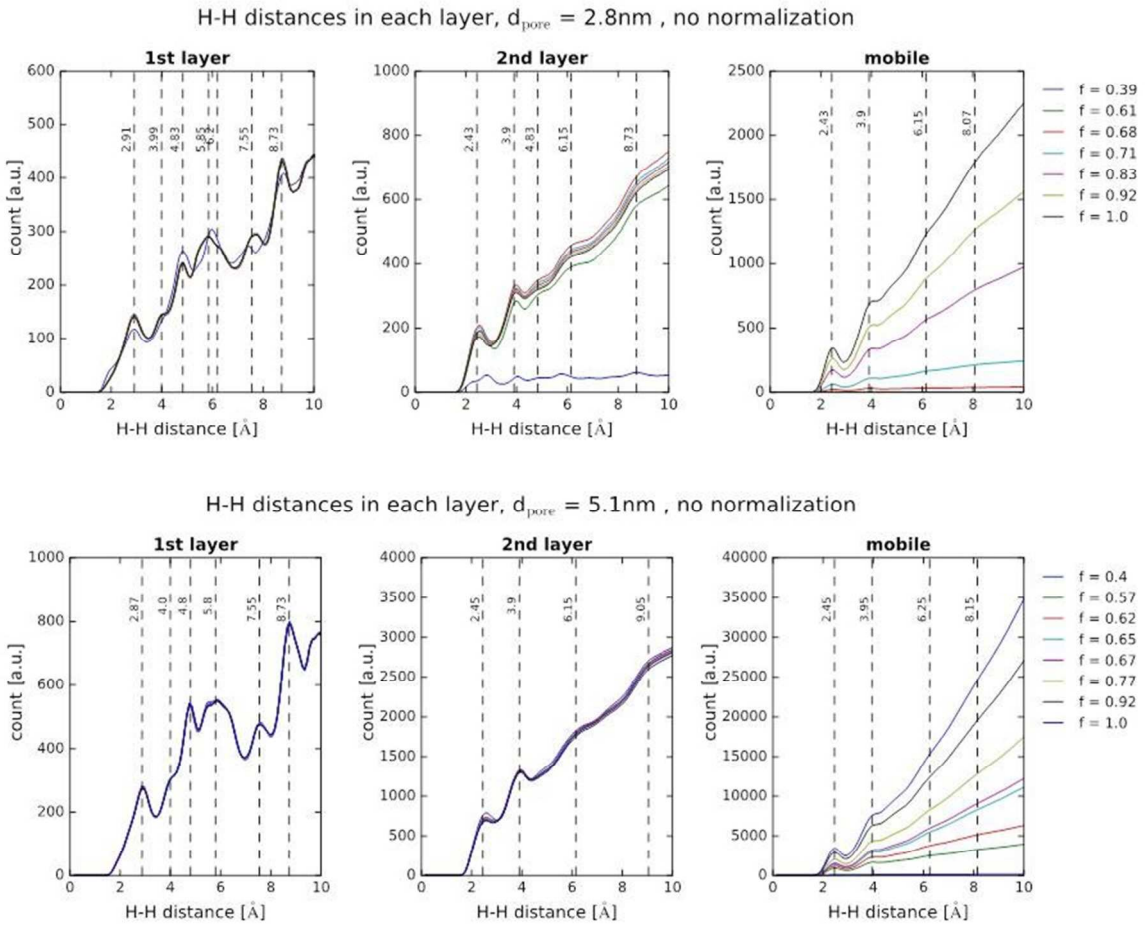

Figure S1 Distance between intermolecular H atoms for molecules in the first, second, and mobile layer (panels left, center, and right respectively). Results corresponds to MD simulations of a 2.8 (upper panels) and 5.1 nm (lower panels) pore with different water content, as indicated in the legends.

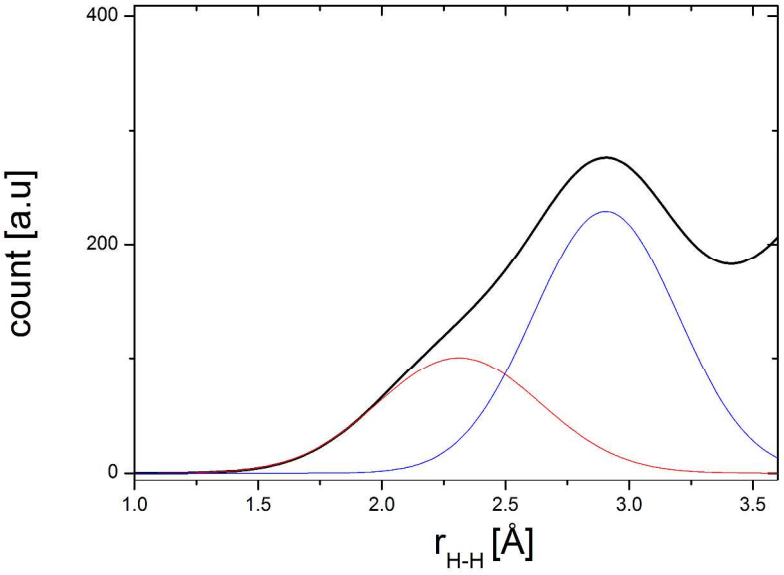

Figure S2 Distance between intermolecular H atoms for molecules in the first layer obtained from MD, and the gaussian deconvolution.

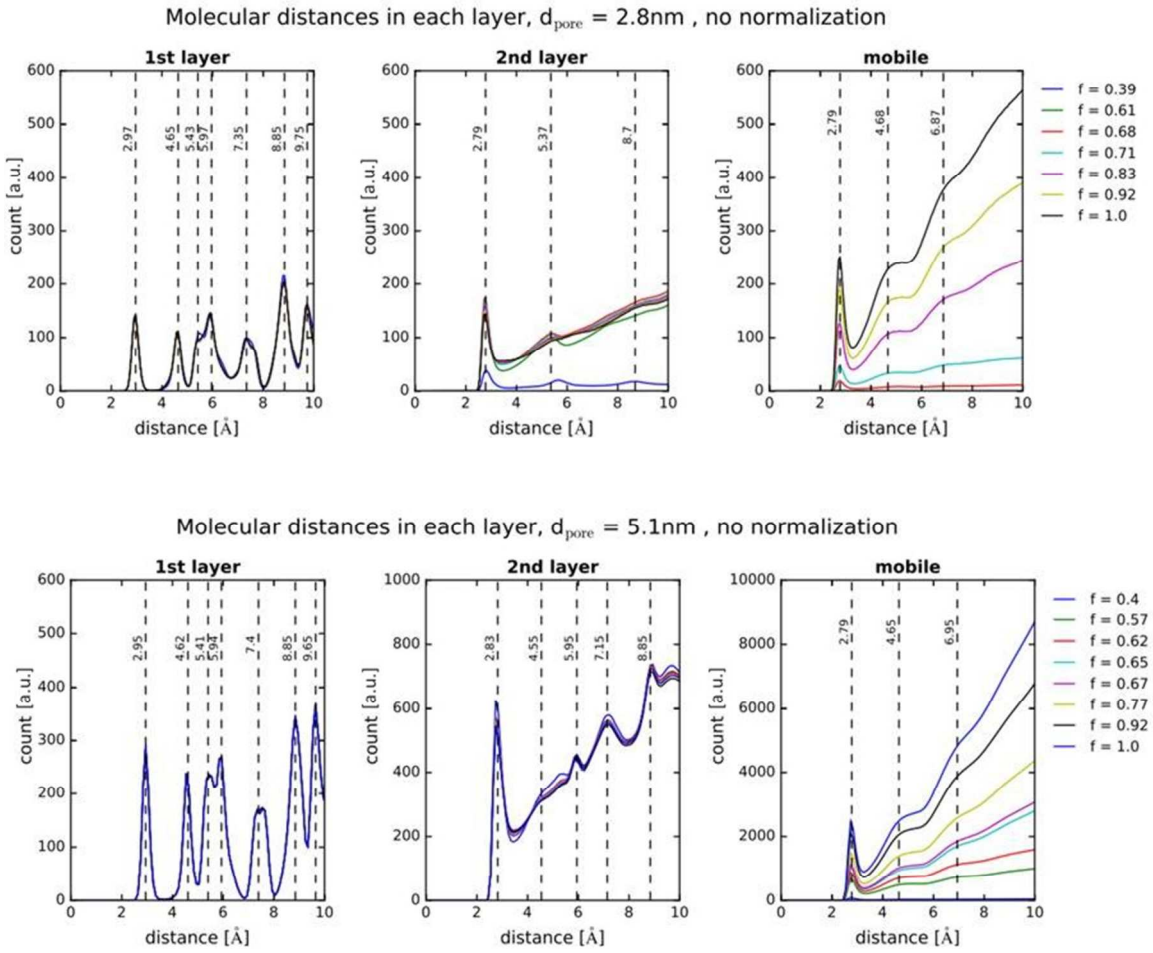

Figure S3 Distance between intermolecular O atoms for molecules in the first, second, and mobile layer (panels left, center, and right respectively). Results corresponds to MD simulations of a 2.8 (upper panels) and 5.1 nm (lower panels) pore with different water content, as indicated in the legends.

DQ-NMR

The DQ-NMR experiment is composed by three main blocks: Excitation-Evolution-Reconversion. The complete DQ sequence scheme used is: $[90°_x\text{-}\tau\text{-}90°_x\text{-}t_1\text{-}90°_y\text{-}\tau\text{-}90°_{-y}\text{-}t_f\text{-}90°_x]$[1]. During the first block, coherences of order two (which comprise two coupled spins) are excited with the application of two 90 degree pulses. Then, the excited coherences freely evolve during a fixed time t_1. The double quantum coherences are not NMR observables and their detection is achieved in an indirect manner by the reconversion to observable magnetization in the third part of the experiment, again with two 90 degree pulses. The receiver phase is cycled in $\pm\pi$ on each acquisition in order to remove undesired coherences. In Figure S the spectrum for the completely filled sample (sample E) is shown in dotted line, the evolution temporal parameters were set as t_1 =10 μs; t_f =50 μs and τ=35μs. Two different contributions to the spectrum are easily distinguished.

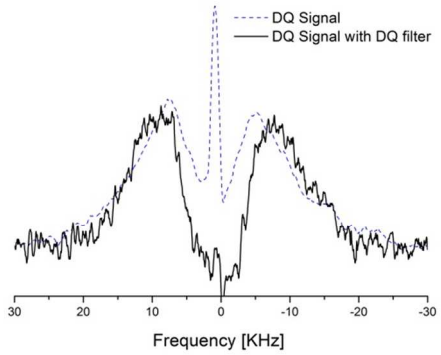

Figure S4 DQ Spectra for sample E, without and with DQ filter application.

The broader contribution in the spectrum in Figure S corresponds to those protons with a large dipolar coupling, i.e. very close to each other. The narrower contribution corresponds to the more mobile water. In order to remove the influence of the more mobile water a DQ filter is applied before the proper DQ sequence[2]. The spectrum obtained after the DQ filter (the filter time was set as τ_f=35μs) is the one shown in straight line in Figure S, where only the broad contribution remains.

By repeating the DQ experiment incrementing the mixing time τ, a build up of the double quantum coherence is obtained[3,4]. The build up curves were recorded after de DQ filter and shown in Figure S for samples A, B and E. The signal S_{DQ} shown in Fig. S4 is normalized

according to a standard normalization process[5]. For the mentioned normalization, a second experiment, without receiver cycling was performed in order to get rid of the dipolar encoded longitudinal magnetization from the DQ signal.

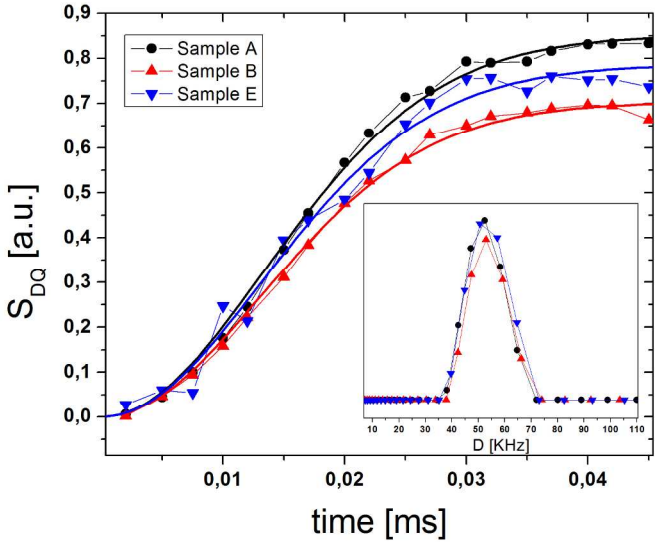

Figure S5 Filter DQ build up curves for samples A,B and E. Inset: Dipolar distribution obtained by Inverse Laplace transformation with kernel function 0.5*(1-exp(-t^2*D^2))

By means of an inverse Laplace transform[6,7] the build up curves, were fitted with an inverted Gaussian function, based on static second moment approximations[2], to the function $S_{DQ} = 0.5 * (1 - \exp(-t^2 D^2))$. In the former equation, the parameter D indicates the residual dipolar coupling. From the Laplace Transform a distribution of residual dipolar constant is obtained, see inset in Figure S. This distribution corresponds to the contribution of different intermolecular spin pair couplings.

The residual dipolar coupling is related to the intermolecular distance[8] as $D = \frac{\mu_0}{4\pi}\frac{\gamma^2\hbar}{r^3}$. This expression was used for the rescaling of the distribution of dipolar couplings to intermolecular distances, shown in Fig. 4 in the report.

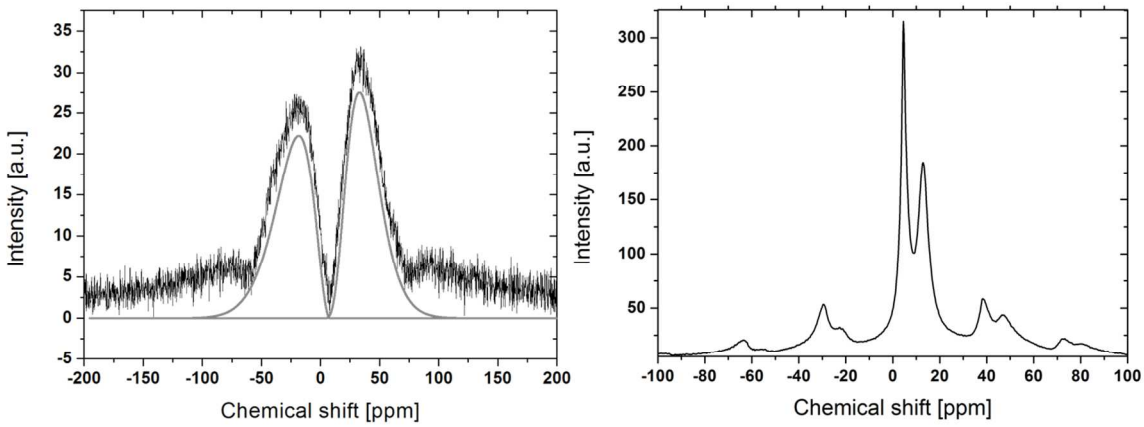

Figure S6. Left: DQ spectrum of sample A and its fitting function, shown in gray color. Right: MAS spectrum obtained at 10 kHz spinning rate. The doublet corresponding to the second layer is more evident in the rotational bands, where the mobile contribution is lower.

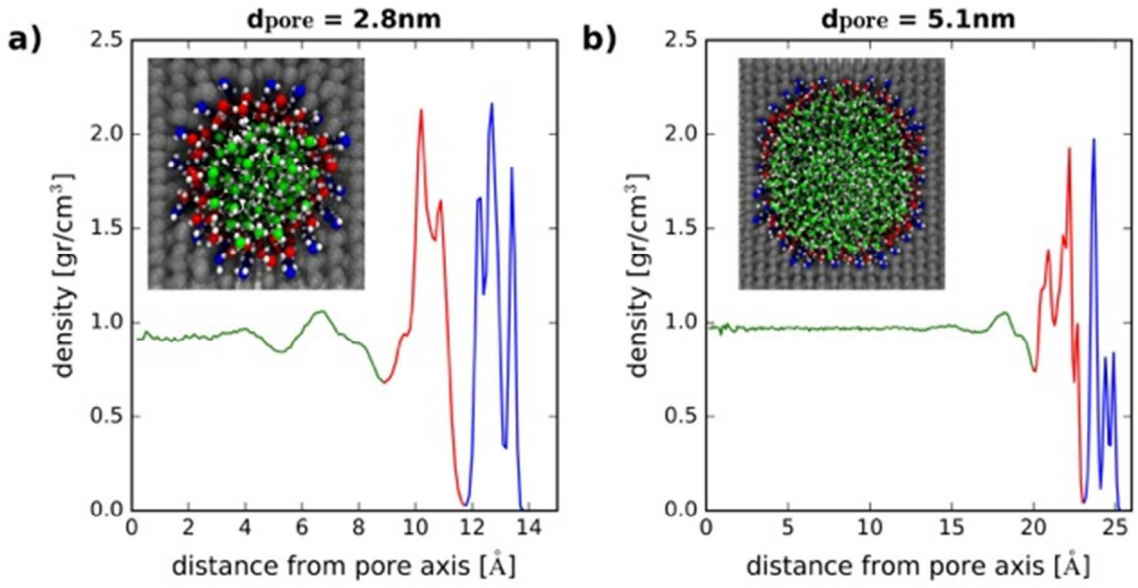

Figure S7. Radial density profiles for the a) 2.8 nm and b) 5.1 nm pores at 100% filling. Red, blue and green lines correspond to water molecules in the first, second, and mobile layers respectively, as also depicted in the inserts showing snapshots of the final configurations at 300K. Adapted with permission from Ref [9]. Copyright 2013 American Chemical Society.

References

(1) Voda, M. A.; Demco, D. E.; Perlo, J.; Orza, R. A.; Blümich, B. Multispin Moments Edited by Multiple-Quantum NMR: Application to Elastomers. *J. Magn. Reson.* **2005**, *172*, 98–109.

(2) Saalwächter, K. Proton Multiple-Quantum NMR for the Study of Chain Dynamics and Structural Constraints in Polymeric Soft Materials. *Prog. Nucl. Magn. Reson. Spectrosc.* **2007**, *51*, 1–35.

(3) Baum, J.; Munowitz, M.; Garroway, a. N.; Pines, A. Multiple-Quantum Dynamics in Solid State NMR. *J. Chem. Phys.* **1985**, *83*, 2015.

(4) Ernst, R. R.; Bodenhausen, G.; Wokaun, W. *Principles of Nuclear Magnetic Resonance in One and Two Dimensions*; Oxford, O., Ed.; Oxford, 1990.

(5) Acosta, R. H.; Monti, G. A.; Villar, M. A.; Vallés, E. M.; Vega, D. A. Transiently Trapped Entanglements in Model Polymer Networks. *Macromolecules* **2009**, *42*, 4674–4680.

(6) Bell, J. B.; Tikhonov, A. N.; Arsenin, V. Y. Solutions of Ill-Posed Problems. *Math. Comput.* **1978**, *32*, 1320.

(7) Provencher, S. W. A Constrained Regularization Method for Inverting Data Represented by Linear Algebraic or Integral Equations. *Comput. Phys. Commun.* **1982**, *27*, 213–227.

(8) Levitt, M. H. *Spin Dynamics: Basics of Nuclear Magnetic Resonance, 2nd Edition.*; 2009.

(9) Solveyra, E. G.; de la Llave, E.; Molinero, V.; Soler-Illia, G. J. A. A.; Scherlis, D. A. Structure, Dynamics, and Phase Behavior of Water in TiO_2 Nanopores. *J. Phys. Chem. C* **2013**, *117*, 3330–3342.